Information Sciences 370–371 (2016) 725–742

Contents lists available at ScienceDirect

Information Sciences

journal homepage: www.elsevier.com/locate/ins

Robust control for a networked direct-drive linear motion control system: Design and experiments☆

Li Qiu[a], Yang Shi[b,*], Jianfei Pan[a], Bugong Xu[c], Huxiong Li[d]

[a] College of Mechatronics and Control Engineering, Shenzhen University, Shenzhen 518060, China
[b] Department of Mechanical Engineering, University of Victoria, PO Box 1700, Stn. CSC, Victoria, BC V8W 2Y2, Canada
[c] School of Automation Science and Engineering, South China University of Technology, Guangzhou 510641, China
[d] School of New Media, Zhejiang University of Media and Communications, No. 998 Xueyuan Street, Xiasha Higher Education Zone, Hangzhou 310018, China

ARTICLE INFO

Article history:
Received 16 January 2015
Revised 3 February 2016
Accepted 8 February 2016
Available online 13 February 2016

Keywords:
Networked control systems
Robust control
Linear switched reluctance machine
Network-induced random time delays

ABSTRACT

This paper investigates the robust control method for networked dynamic systems and its application for a direct-drive linear motion control system in a network environment. The unavoidable network-induced random delays are modeled as Markov chains. The control object of the linear motion control system in this study is a double-sided linear switched reluctance machine (DLSRM). To tackle the inherent uncertainties in the DLSRM, a robust control strategy is designed by proposing a new Lyapunov function and applying the free-weighting matrix technique. A state feedback robust controller is designed such that the closed-loop direct-drive linear motion control system over a network is stochastically robust stable. The robust controller can be conveniently obtained by solving a set of linear matrix inequalities. The numerical simulation of an angular positioning system is presented to illustrate the effectiveness of the proposed robust control method. Furthermore, the experimental tests on the networked direct-drive linear motion control system verify the practicability of the proposed method.

© 2016 Elsevier Inc. All rights reserved.

1. Introduction

With the rapid development of network communication technologies, networked control systems (NCSs) are becoming increasingly important in industrial processes because of low cost, high flexibility, reduced wiring, simple installation and maintenance, and so on. Hence, NCSs are applied in a broad range of areas, such as in vehicles, aircrafts, spacecrafts, manufacturing plants, and remote surgeries [4,21,32,49,51]. However, the insertion of communication networks into feedback control loops introduces several challenging topics, such as constraints on communication bandwidth [1,6,7,39,42], network-induced time delays [2,3,5,9–12,14,20,27,28,31,33–35,45,50], packet dropouts [9,11,15,24,25,28,35,44], signal quantization [19], optimal denial-of-service attack scheduling [48], distributed synchronization [37,46], fault detection [18,41,47], and fuzzy control [8]. Thus, the network characteristics must be considered explicitly in the NCS design.

☆ This work is supported by the National Natural Science Foundation of China (Grant Nos. 61403258, 61473116, 51477103, 61174070), by the Natural Science Foundation of Guangdong Province (Grant nos. S2013040016183, S2014A030313564, S2015A010106017), by the Science and Technology Development Foundation of Shenzhen Government (Grant no. JCYJ20140418182819153), and partially by the Zhejiang Province International Cooperation Foundation (2012C24019) and the Zhejiang Province Natural Science Foundation (LY13F020023).

* Corresponding author. Tel.: +1 2508533178.
E-mail address: yshi@uvic.ca, yangshi.uvic@gmail.com (Y. Shi).

http://dx.doi.org/10.1016/j.ins.2016.02.022
0020-0255/© 2016 Elsevier Inc. All rights reserved.

Time delay is one of the major issues in communication networks and it may lead to system instability and performance deterioration. The Lyapunov functional approach with the help of the linear matrix inequalities (LMIs) technique can present simple and delay-independent results for the considered NCS with time delays. By contrast, error in the modeling process or the changing operating condition of a practical application results in the difficulty for an exact mathematical model [40]. Therefore, the robust control problems of NCSs have received considerable attention oeing to the excellent ability of NCSs to balance the robustness and performance of a system with an inexact mathematical model. In [38], the robust stability analysis of the wireless NCS with stochastic time delays and packet dropouts is investigated by the robust model predictive controller technique. In [43], the composite adaptive tracking control for a class of uncertain nonlinear systems in strict-feedback forms are studied on the basis of the network control framework. In [17], the infinite-horizon optimal-robust guaranteed cost control of continuous-time uncertain nonlinear systems is investigated by using a neural-network-based online solution of Hamilton–Jacobi–Bellman equation. In [52], a robust distributed model predictive control is proposed for uncertain NCSs with time delays. In [29], the guaranteed cost control problem is studied for the NCS with uncertain parameters, random packet dropouts, and time delays. In particular, robust control is important for the NCS based industrial applications because the mathematical models suitable for industrial objects are often inaccurate, and the inaccuracy of the model can be compensated by uncertain but bounded system parameters.

The robust control problems of NCSs and their industrial applications are more challenging than stabilization problems, though most existing work focuses on the stabilization and robust control problems of NCSs. In this paper, a robust control scheme is first developed to design a state feedback controller for the NCS with uncertain parameters, random forward and backward communication links with time delays. Then the application of the proposed control scheme to a direct-drive linear motion control system over a communication network is investigated. Current research on DLSRM-based direct-drive motion control systems mainly concentrates on the controller design without the introduction of any communication network. For example, a nonlinear proportion-derivative position controller based on the tracking differentiator is introduced for the DLSRM-based motion control system to achieve an improved dynamic response [16]. An adaptive position regulator is proposed to combat the nonlinearities and uncertain control behaviors of the DLSRM in [22]. However, the aforementioned methods need to be reevaluated when the DLSRM exists over a communication network with time delays and this motivates the research in this paper. On the basis of the above analysis, this study aims to solve the robust state feedback control problem for the networked DLSRM system by incorporating parameter uncertainties and the random network-induced time delays that exist in both the forward and feedback communication links. The contributions of this paper are mainly three-fold. First, a new Lyapunov functional is constructed for the NCS with uncertain parameters and random networked-induced time delays. Sufficient conditions are obtained for the NCS by using the free-weighting matrix technique. Second, a robust state feedback controller is developed. Compared with the robust output feedback controller in [27], the proposed control scheme improves the dynamic behaviors and reduces computational complexity. Finally, the robust control scheme is applied to the networked direct-drive linear motion control system with uncertain parameters and random networked-induced time delays.

The rest of this paper is organized as follows. Section 2 presents the problem formulation of the NCS and objective. Section 3 inspects the robust stability analysis and robust controller design for the NCS. Section 4 presents the numerical simulations and experimental tests. Conclusions are given in Section 5 and an appendix is provided for the formal proofs of the results in the main body.

Notations: Let $\mathbb{R}^n$ and $\mathbb{R}^{n\times m}$ denote the n dimensional Euclidean space and the set of all $n \times m$ real matrices, respectively. The notation $A > 0$ ($A < 0$) indicates that A is a real symmetric positive (negative) definite matrix. Superscripts "T" and "-1" stand for matrix transposition and matrix inversion, respectively. I and 0 denote the identity and zero matrices, respectively, with appropriate dimensions. $\mathbb{E}[\cdot]$ stands for the mathematical expectation, and diag$\{A, B\}$ stands for a block-diagonal matrix of A and B. $\|\cdot\|_2$ denotes 2-norm of a matrix or vector. sym$\{A\}$ is used to denote the expression $A + A^T$. The symbol $*$ indicates a symmetric term in symmetric entries. For the sake of notation convenience, we will use the notation x_k for $x(k)$.

2. Problem statement

The networked direct-drive linear motion control system is shown in Fig. 1.

Considering the network-induced random delays in both forward and feedback communication links, the discrete model of the control object DLSRM can be denoted as follows:

$$\begin{cases} x_{k+1} = (A + \Delta A)x_k + (B + \Delta B)u_k, \\ \begin{bmatrix} \Delta A & \Delta B \end{bmatrix} = D\Delta_k \begin{bmatrix} E_1 & E_2 \end{bmatrix}, \\ \Delta_k^T \Delta_k \le I, \end{cases} \tag{1}$$

where $x_k \in \mathbb{R}^n$ is the system state vector, $u_k \in \mathbb{R}^m$ is the control input vector, and A, B, D, E_1, and E_2 are known real constant matrices with appropriate dimensions. Δ_k is an unknown matrix that represents time-varying norm-bound parameter uncertainties.

Both the controller and plant nodes are connected via the forward and feedback communication network links. We assume that the sensor, actuator (or linear encoder, driver), and controller are clock-driven and synchronized, similar to that in [32]. d_k and τ_k stand for the network-induced time delays of the forward and feedback communication links, respectively.

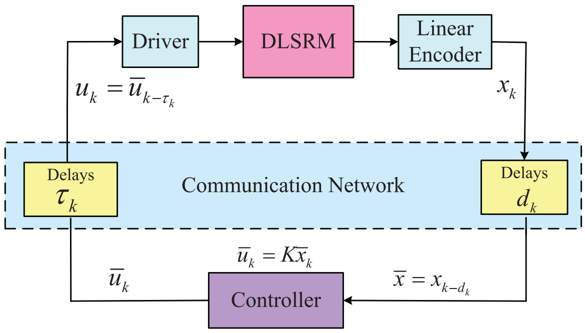

Fig. 1. Structure of the networked DLSRM system.

Both d_k and τ_k are bounded:

$$0 \le \underline{d} \le d_k \le \bar{d}, \quad 0 \le \underline{\tau} \le \tau_k \le \bar{\tau}, \tag{2}$$

where $\underline{d} = \min\{d_k\}$, $\bar{d} = \max\{d_k\}$, $\underline{\tau} = \min\{\tau_k\}$, $\bar{\tau} = \max\{\tau_k\}$. To be precise, the values of the above random time delays are continuous. However, the clock-driven controller and drive only accept data at discrete time instants [32]. Thus, d_k and τ_k take values in discrete sets. Random networked-induced time delays d_k and τ_k are modeled as two homogeneous Markov chains. The main advantage of the Markov model is that the dependence between delays is considered, which is caused by the fact that the current time delays are frequently related to the previous delays in real networks. The random time delays d_k and τ_k take values in the finite set $\mathbb{M} = \{0, 1, 2, ..., M\}$ and $\mathbb{N} = \{0, 1, 2, ..., N\}$, respectively, and the transition probability matrices are $\pi = [\pi_{ij}]$ and $\lambda = [\lambda_{mn}]$, respectively. Thus, d_k and τ_k jump from mode i to j and from mode m to n (in this paper, Markov mode i, j, m, and n stand for the time delay steps), respectively, with probabilities π_{ij} and λ_{mn}, which are defined as follows:

$$\begin{cases} \pi_{ij} = Pr\{d_{k+1} = j | d_k = i\}, \\ \lambda_{mn} = Pr\{\tau_{k+1} = n | \tau_k = m\}, \end{cases} \tag{3}$$

where $\pi_{ij} \ge 0$, $\lambda_{mn} \ge 0$ and

$$\sum_{j=0}^{M} \pi_{ij} = 1, \quad \sum_{n=0}^{N} \lambda_{mn} = 1, \tag{4}$$

for $\{i, j \in \mathbb{M}\}$, $\{m, n \in \mathbb{N}\}$.

Remark 1. The network-induced packet dropouts and disorder can be formulated from time delays. If a data packet is lost or a disorder occurs, the most recently arrived data packet will be applied. Thus, packet dropouts can be treated as the upper bound of time delays or infinite delays [13,30]. The disorder can be treated as the jump between different time delay modes. The current problem formulation can accommodate packet dropouts and disorders. Thus, the packet dropouts and disorder problems can be included in the random time delays.

The objective of this paper is to achieve a robust control performance for the NCS and apply the proposed method to a DLSRM over a communication network (Fig. 1). Assuming that the system state is measurable, we adopt a mode-independent state feedback controller:

$$\bar{u}_k = K\bar{x}_k, \tag{5}$$

where K is the mode-independent state feedback controller gain. By substituting (5) into (1), we can obtain the closed-loop system:

$$\begin{cases} x_{k+1} = \hat{A}x_k + \hat{B}Kx_{k-\eta_k}, \\ x_{k_0} = \varphi_0, k_0 = -\bar{d} - \bar{\tau}, -\bar{d} - \bar{\tau} + 1, ..., 0, \end{cases} \tag{6}$$

where

$$\hat{A} = A + \Delta A, \quad \hat{B} = B + \Delta B, \quad \eta_k = \tau_k + d_{k-\tau_k}.$$

ΔA and ΔB are defined in (1), φ_0 is the initial condition.

Remark 2. Many studies have focused on the design of a mode-dependent controller (the controller gain depends on the information of time delays). For example, the mode-dependent dynamic output feedback controller has been investigated in [33] and the delay information of $d_{k-\tau_k-1}$ is incorporated into the dynamic output feedback controller design. In addition, the multi-step jump of Markov chains is involved in the closed-loop system. In this paper, we adopt a mode-independent state feedback controller (5) which can avoid controller gain switching in high frequency, following the multi-mode of Markov chain d_k and τ_k induced by the communication network that exists in the linear motion control system.

Remark 3. The DLSRM model is obtained by on-line experiments in this paper. Since it is difficult to obtain the accurate mathematical model [23], the parameter uncertainties are used to compensate the mathematical model. The methods of dealing with the uncertain parameters in [28,29] provide a guidance for this paper.

3. Robust stability analysis and controller design

3.1. Robust stability analysis

The criteria of ensuring stochastic robust stability and the design of the state feedback robust controller gain K for the closed-loop system are derived from model (6). For this purpose, the definitions of stochastic stability and a lemma are provided to cope with the uncertainties of the system parameters.

Definition 1 ([34]). The closed-loop system given by (6) is said to be stochastically stable if for every initial mode $x_0 = x(0)$, $d_0 = d(0) \in \mathbb{M}$, and $\tau_0 = \tau(0) \in \mathbb{N}$, there exists a finite $\mathcal{W} > 0$ such that the following inequality holds:

$$\mathbb{E}\left\{ \sum_{k=0}^{\infty} \|x_k\|^2 | x_0, d_0, \tau_0 \right\} < x_0^T \mathcal{W} x_0. \tag{7}$$

Lemma 1 ([26]). *Let Σ_1, Σ_2, and Σ_3 be the real matrices of appropriate sizes, with $\Sigma_1 = \Sigma_1^T$. Then,*

$$\Sigma_1 + \Sigma_2 \Delta_k \Sigma_3 + \Sigma_3^T \Delta_k^T \Sigma_2^T < 0$$

holds for all Δ_k and satisfies $\Delta_k^T \Delta_K \le I$ if and only if for some $\varepsilon > 0$,

$$\Sigma_1 + \varepsilon \Sigma_2 \Sigma_2^T + \varepsilon^{-1} \Sigma_3^T \Sigma_3 < 0.$$

Theorem 1. *For the closed-loop system in (6) with the random but bounded time delay $d_k \in \begin{bmatrix} \underline{d} & \bar{d} \end{bmatrix}$ and $\tau_k \in \begin{bmatrix} \underline{\tau} & \bar{\tau} \end{bmatrix}$, if matrices $P_{i,\,m} > 0$, $Q > 0$, $R > 0$, $\mathbb{U} = \begin{bmatrix} \mathcal{U}_1 & \mathcal{U}_2 & \mathcal{U}_3 \end{bmatrix}$ exist for modes $\{i, j\} \in \mathbb{M}$ and $\{m, n\} \in \mathbb{N}$, then K satisfies the following matrix inequality*

$$\Theta_{i,m} = \mathrm{sym}\{\bar{\mathbb{U}}^T \mathbb{A}\} + \Gamma_{i,m} < 0, \tag{8}$$

where

$$\begin{aligned}
\bar{\mathbb{U}} &= \begin{bmatrix} \mathcal{U}_1 & \mathcal{U}_2 & \mathcal{U}_3 & 0 \end{bmatrix},\\
\mathbb{A} &= \begin{bmatrix} \hat{A} - I & -I & \hat{B}K & 0 \end{bmatrix},\\
\Gamma_{i,m} &= \begin{bmatrix} \Xi_{11} & \bar{P}_{i,m} & R & 0 \\ \bar{P}_{i,m} & \Xi_{22} & 0 & 0 \\ R & 0 & \Xi_{33} & R \\ 0 & 0 & R & \Xi_{44} \end{bmatrix},\\
\Xi_{11} &= \bar{P}_{i,m} + P_{i,m} + (\bar{\eta} - \underline{\eta} + 2)Q - R,\\
\Xi_{22} &= \bar{P}_{i,m} + \bar{\eta}^2 R, \quad \Xi_{33} = -Q - 2R, \quad \Xi_{44} = -Q - R,\\
\bar{P}_{i,m} &= \sum_{j=0}^{M} \sum_{n=0}^{N} \pi_{ij} \lambda_{mn} P_{j,n}, \quad \bar{\eta} = \bar{d} + \bar{\tau}, \quad \underline{\eta} = \underline{d} + \underline{\tau},
\end{aligned}$$

with $\hat{A}$ and $\hat{B}$ defined in (6).

Thus, the closed-loop system in (6) with the state feedback controller (5) exhibits stochastic stability.

Proof. See Appendix A. □

Remark 4. The equation in (8) from Theorem 1 provides sufficient stability conditions for the closed-loop system (6). However, Eq. (8) contains uncertain but bounded Δ_k. So condition (8) cannot account for all admissible uncertain matrices Δ_k. To address this issue, the equivalent description is given as follows.

Theorem 2. *For the closed-loop system in (6) with the random but bounded time delay $d_k \in \begin{bmatrix} \underline{d} & \bar{d} \end{bmatrix}$ and $\tau_k \in \begin{bmatrix} \underline{\tau} & \bar{\tau} \end{bmatrix}$, if scalar $\varepsilon > 0$ and matrices $P_{i,\,m} > 0$, $Q > 0$, $R > 0$, $\mathbb{U} = \begin{bmatrix} \mathcal{U}_1 & \mathcal{U}_2 & \mathcal{U}_3 \end{bmatrix}$ exist for modes $\{i, j\} \in \mathbb{M}$ and $\{m, n\} \in \mathbb{N}$, then K satisfies the following matrix inequality*

$$\begin{bmatrix} -\varepsilon I & \Upsilon_{12} \\ * & \Upsilon_{22} \end{bmatrix} < 0, \tag{9}$$

where

$$\Upsilon_{12} = [E_1 \quad 0 \quad E_2K \quad 0 \ ],$$
$$\Upsilon_{22} = \Gamma_{i,m} + \mathrm{sym}\{[\mathcal{U}_1 \quad \mathcal{U}_2 \quad \mathcal{U}_3 \quad 0]^T[A-I \quad -I \quad BK \quad 0]\} + \varepsilon[\mathcal{U}_1 \quad \mathcal{U}_2 \quad \mathcal{U}_3 \quad 0]^T DD^T[\mathcal{U}_1 \quad \mathcal{U}_2 \quad \mathcal{U}_3 \quad 0 \ ],$$

and $\Gamma_{i,\,m}$ *is defined in Theorem 1.*

Thus, system (1) with the state feedback controller (5) exhibits robust stochastic stability for all admissible uncertainties.

Proof. In Theorem 1

$$\begin{aligned}\Theta_{i,m} &= \mathrm{sym}\{\bar{\mathbb{U}}^T\mathbb{A}\} + \Gamma_{i,m}\\ &= \mathrm{sym}\{[\mathcal{U}_1 \quad \mathcal{U}_2 \quad \mathcal{U}_3 \quad 0]^T[\hat{A}-I \quad -I \quad \hat{B}K \quad 0]\} + \Gamma_{i,m}\\ &= \mathrm{sym}\{[\mathcal{U}_1 \quad \mathcal{U}_2 \quad \mathcal{U}_3 \quad 0]^T[A-I \quad -I \quad BK \quad 0]\} + \Gamma_{i,m}\\ &\quad + \mathrm{sym}\{[\mathcal{U}_1 \quad \mathcal{U}_2 \quad \mathcal{U}_3 \quad 0]^T[D\Delta_kE_1 \quad 0 \quad D\Delta_kE_2K \quad 0]\}\\ &= \mathrm{sym}\{[\mathcal{U}_1 \quad \mathcal{U}_2 \quad \mathcal{U}_3 \quad 0]^T[A-I \quad -I \quad BK \quad 0]\} + \Gamma_{i,m}\\ &\quad + \mathrm{sym}\{[\mathcal{U}_1 \quad \mathcal{U}_2 \quad \mathcal{U}_3 \quad 0]^T D\Delta_k[E_1 \quad 0 \quad E_2K \quad 0 \ ]\} < 0.\end{aligned}$$

According to Lemma 1 and on the basis of the Schur complement, Theorem 2 can be obtained, thus completing the proof. □

3.2. Robust controller design

This section focuses on the design of the state feedback controller (5) to stabilize the closed-loop system (6) by the linear matrix inequality approach.

Theorem 3. *For the closed-loop system in (6) with the random but bounded time delay* $d_k \in \left[\underline{d} \quad \bar{d}\right]$ *and* $\tau_k \in \left[\underline{\tau} \quad \bar{\tau}\right]$, *if scalar* $\varepsilon > 0$, *tuning parameters* $\vartheta_1 > 0$ *and* $\vartheta_2 > 0$, *and matrices* $X > 0$, $\hat{P}_{i,m} > 0$, $\hat{Q} > 0$, $\hat{R} > 0$ *exist for modes* $\{i, j\} \in \mathbb{M}$ *and* $\{m, n\} \in \mathbb{N}$, *then Y exists such that*

$$\begin{bmatrix} -\varepsilon I & \hat{\Upsilon}_{12} \\ * & \hat{\Upsilon}_{22}\end{bmatrix} < 0, \tag{10}$$

where

$$\hat{\Upsilon}_{12} = \left[E_1X \quad 0 \quad \vartheta_2E_2Y \quad 0\right],$$
$$\hat{\Upsilon}_{22} = \hat{\Gamma}_{i,m} + \mathrm{sym}\{\hat{\Pi}\} + \varepsilon\mathcal{I}^TDD^T\mathcal{I},$$
$$\hat{\Gamma}_{i,m} = \begin{bmatrix} \hat{\Xi}_{11} & \vartheta_1\hat{\bar{P}}_{i,m} & \vartheta_2\hat{R} & 0\\ * & \hat{\Xi}_{22} & 0 & 0\\ * & * & \hat{\Xi}_{33} & \vartheta_2\hat{R}\\ * & * & * & \hat{\Xi}_{44}\end{bmatrix},$$
$$\hat{\Pi} = \mathcal{I}^T\mathcal{A}, \mathcal{I} = \left[I \quad I \quad I \quad 0\right],$$
$$\mathcal{A} = \left[(A-I)X \quad -\vartheta_1X \quad \vartheta_2BY \quad 0\right],$$
$$\hat{\Xi}_{11} = \hat{\bar{P}}_{i,m} + \hat{P}_{i,m} + (\bar{\eta} - \underline{\eta} + 2)\hat{Q} - \hat{R},$$
$$\hat{\Xi}_{22} = \vartheta_1^2(\hat{\bar{P}}_{i,m} + \bar{\eta}^2\hat{R}),\ \hat{\Xi}_{33} = -\vartheta_2(\hat{Q} + \hat{R}),\ \hat{\Xi}_{44} = -\hat{Q} - \hat{R},$$
$$\hat{\bar{P}}_{i,m} = \sum_{j=0}^{M}\sum_{n=0}^{N}\pi_{ij}\lambda_{mn}\hat{P}_{j,n}.$$

Thus, the closed-loop system (6) has robust stochastic stability, $\bar{u}_k = K\bar{x}_k$ *is a state feedback controller of system (1) with gain* $K = YX^{-1}$.

Proof. Let $\varrho_{im} = \mathrm{diag}\{I, X_{i,m}, \vartheta_1X_{i,m}, \vartheta_2X_{i,m}, X_{i,m}\}$, $\mathcal{U}_1^{-1} = X_{i,m}$, $\mathcal{U}_2^{-1} = \vartheta_1X_{i,m}$, and $\mathcal{U}_3^{-1} = \vartheta_2X_{i,m}$, where $\vartheta_1 > 0$, and $\vartheta_2 > 0$ are known tuning parameters. We restrict $X_{i,\,m}$ to be the same for all $\{i, m\}$ (namely $X_{i,m} = X$), and give the following notations:

$$\hat{P}_{i,m} = X^TP_{i,m}X,\ \hat{\bar{P}}_{i,m} = X^T\bar{P}_{i,m}X,\ \hat{Q} = X^TQX,\ \hat{R} = X^TRX,\ KX = Y.$$

Pre- and post-multiplying ϱ_{im}^T and ϱ_{im} to (9), respectively, Theorem 3 can be obtained by the Schur complement, thus completing the proof. □

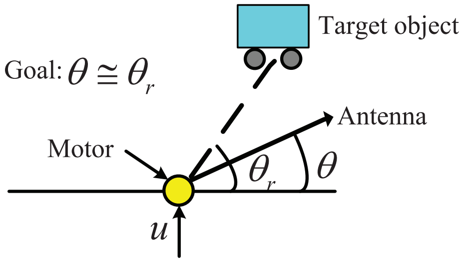

Fig. 2. The angular positioning system.

4. Simulation and experimental results

4.1. Numerical simulation on an angular positioning system

In this subsection, the numerical simulation on an angular positioning system is presented to illustrate the effectiveness of the proposed robust control method.

The classical angular positioning system in Fig. 2 [36] consists of a rotating antenna at the origin of the plane, and the antenna is driven by an electric motor. We assume that the angular position of the antenna as θ (rad), the angular position of the moving object as θ_r (rad), and the angular velocity of the antenna $\dot{\theta}$ (rad s^{-1}) are measurable. The state variables are chosen as $\begin{bmatrix}\theta & \dot{\theta}\end{bmatrix}^T$. The control target is the regulation of the input voltage to the motor to rotate the antenna such that it always points to the direction of the moving object of the plant. The motion of the antenna can be described by the following discrete-time form by using a sampling time of 0.1 s and Euler's first-order approximation for the derivatives.

$$x_{k+1} = \begin{bmatrix}\theta_{k+1} \\ \dot{\theta}_{k+1}\end{bmatrix} = \begin{bmatrix}1 & 0.1 \\ 0 & 1-0.1\partial_k\end{bmatrix} x_k + \begin{bmatrix}0 \\ 0.1\kappa\end{bmatrix} u_k,$$

where $\kappa = 0.787\, rad^{-1} V^{-1} s^{-2}$ and $0.1\, s^{-1} \leq \partial_k \leq 10\, s^{-1}$. The parameter ∂_k is proportional to the coefficient of viscous friction in the rotating parts of the antenna, assuming that $\partial_k = 0.1$. The initial state $x_0 = \begin{bmatrix}0.01 & 0\end{bmatrix}^T$. The state feedback controller is designed for the following values of plant matrices A and B:

$$A = \begin{bmatrix}1 & 0.1 \\ 0 & 0.99\end{bmatrix}, \quad B = \begin{bmatrix}0 \\ 0.0787\end{bmatrix}.$$

The eigenvalues of A are 1 and 0.99, thus, this system is not asymptotically stable. Our purpose is to design a robust controller such that the closed-loop system is stochastically stable with uncertain parameters and random time delays.

To apply Theorem 3 in this example, we assume that the aforementioned system is an uncertain system with norm-bound parameter uncertain matrices D, E_1, and E_2, which has the following values:

$$D = \begin{bmatrix}0 & 0.3 \\ 0.02 & -0.05\end{bmatrix}, \quad E_1 = \begin{bmatrix}0.01 & 0.02\end{bmatrix}, \quad E_2 = 0.03.$$

The random time delays involved in system (6) are assumed to be $d_k = i, i \in \{0, 1, 2\}$ and $\tau_k = m, m \in \{0, 1\}$, and the transition matrices are given as the following values:

$$\pi = \begin{bmatrix}0.5 & 0.2 & 0.3 \\ 0.4 & 0.5 & 0.1 \\ 0.3 & 0.2 & 0.5\end{bmatrix}, \quad \lambda = \begin{bmatrix}0.5 & 0.5 \\ 0.8 & 0.2\end{bmatrix}.$$

Setting the initial state value $x_0 = \begin{bmatrix}0.01 & 0\end{bmatrix}^T$, we give the tuning parameters $\vartheta_1 = 0.8$ and $\vartheta_2 = 50$. The time-varying norm-bound uncertain parameter Δ_k is assumed as follows:

$$\Delta_k = \begin{cases}\begin{bmatrix}0.1\sin(k) \\ 0.3\cos(k)\end{bmatrix}, & 3 \leq k \leq 80 \\ 0, & \text{otherwise.}\end{cases}$$

By applying Theorem 3, we can obtain a scalar $\varepsilon = 9.03 \times 10^{-10}$, and the gain matrix K of controller (5) is expressed as follows:

$$K = \begin{bmatrix}-0.5000 & -1.1251\end{bmatrix}.$$

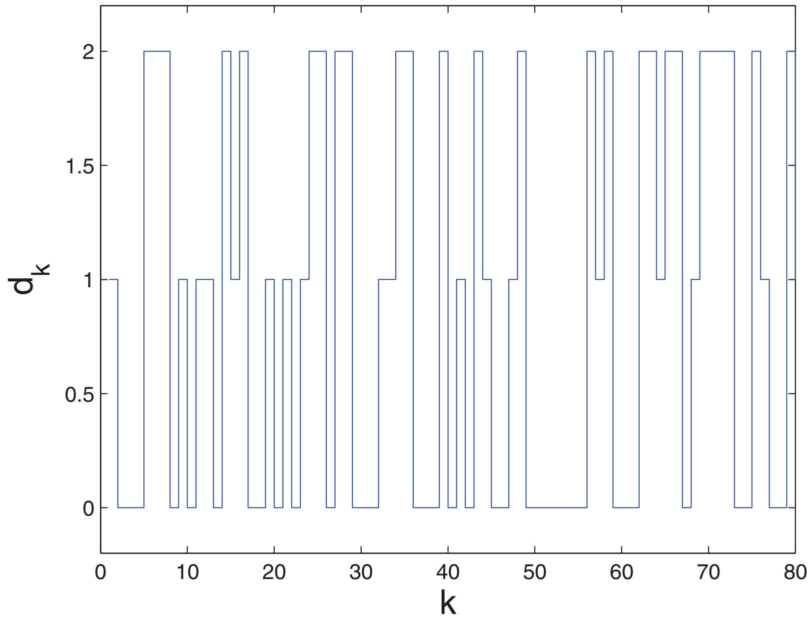

Fig. 3. Time delays d_k.

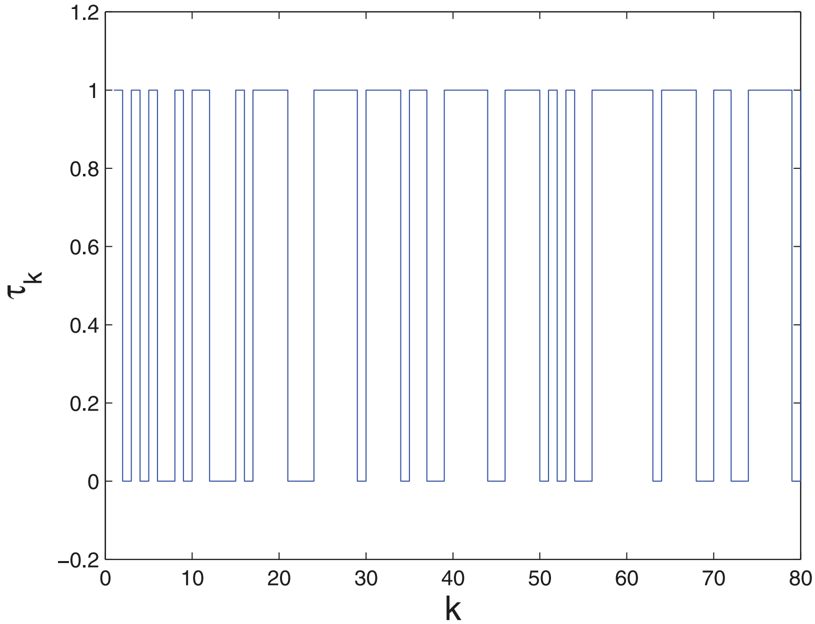

Fig. 4. Time delays τ_k.

Figs. 3 and 4 demonstrate part of the simulation results of the random jumping parameter d_k and τ_k, and they are governed by the corresponding transition probability matrices. Fig. 5 demonstrates the $\|\Delta_k\|_2$ of the time-varying norm-bound uncertain parameters Δ_k, indicating that $\|\Delta_k\|_2 < 1$. The state trajectories are shown in Fig. 6, where two curves show the system under the controller gain K is robust stable.

To further verify the effectiveness of the proposed strategy, a comparative study with the existing method in [27] is addressed. For comparison, a state feedback control is applied to the same angular positioning system in this example. The same initial states $x_0 = \begin{bmatrix} 0.01 & 0 \end{bmatrix}^T$ are set, and the simulation results are shown in Figs. 7 and 8, respectively.

Remark 5. The control performance by using the proposed robust control method for the closed-loop system with random time delays and uncertain parameters can be found in Figs. 7 and 8. It can be seen that the proposed method annihilates

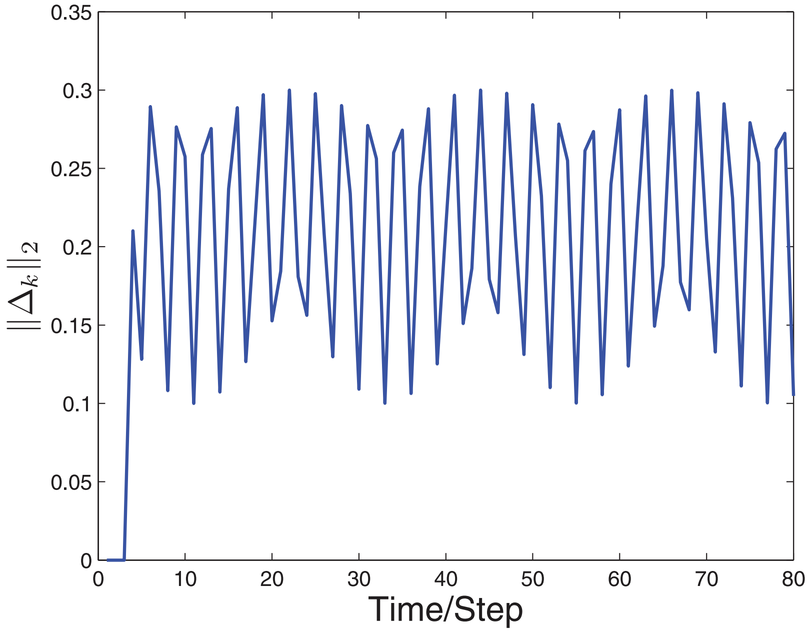

Fig. 5. Values of $\|\Delta_k\|_2$.

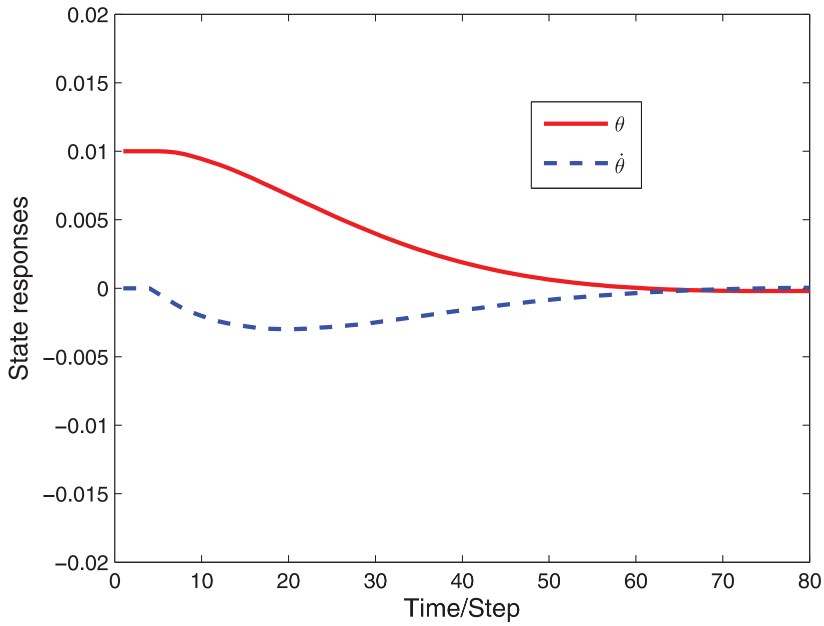

Fig. 6. State trajectories.

overshoots for system state θ and the fluctuations of state $\dot{\theta}$ are also reduced, compared to the output feedback control method [27] for the same system. Since the control systems for electric machines often require less overshoot and fluctuations in the dynamic response, the proposed method is more suitable for the DLSRM system with uncertain parameters.

4.2. Experimental tests on the networked DLSRM

To further illustrate the effectiveness and applicability of the proposed method, the experiment on the networked direct-drive linear motion control system (Fig. 9) is conducted.

The experimental setup consists of a personal computer (PC), DLSRM, dSPACE control platform and driver. The networked controller is implemented in Matlab/Simulink environment on the PC. The setup simulates the situation that the hardware

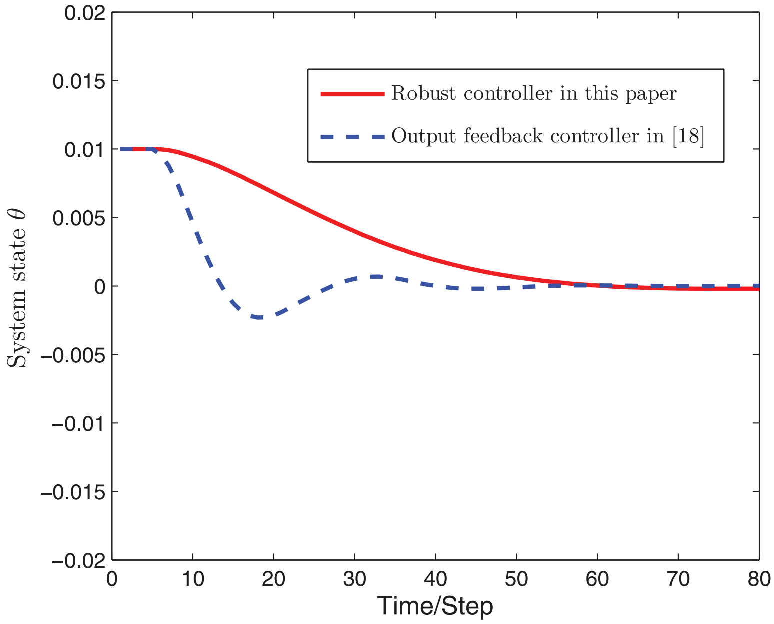

Fig. 7. Response of θ.

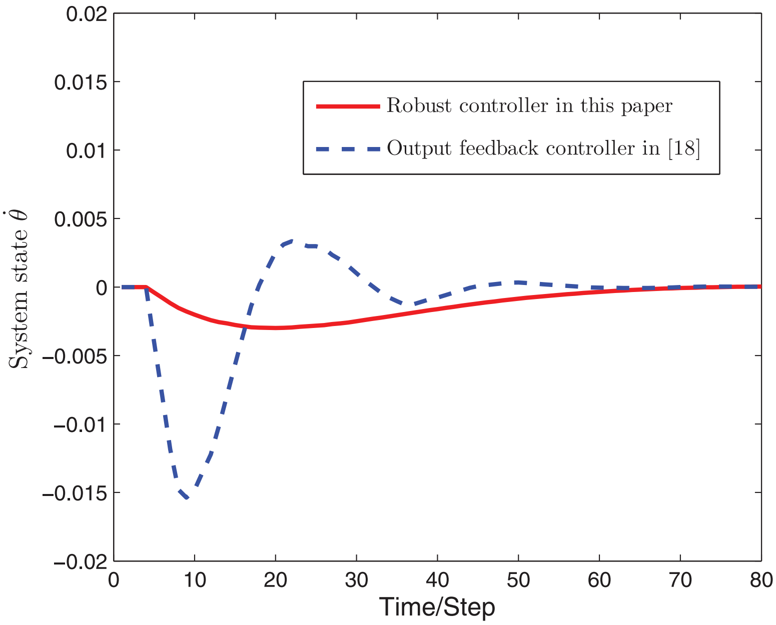

Fig. 8. Response of $\dot{\theta}$.

including the controller, drivers, linear machine and encoder of the DLSRM system is allocated locally. In addition, the PC is the remote monitoring computer collecting the real time position information from the linear encoder (sensor-to-controller) and sending the information to the local controller (controller-to-actuator) simultaneously. As shown in Fig. 9, the control program can be developed under the environment of Matlab/Simulink from the monitoring PC and all control parameters can be modified online. The current drivers for the DLSRM are three commercial amplifiers capable of the inner current regulation with a sampling rate of 20 kHz. Position information is sensed by the linear magnetic encoder with a resolution of 1 μm and the sampling time of the position control loop is 1 ms.

The DLSRM applies the asymmetric linear switched reluctance topology [23]. It is mainly composed of a stator base with three-phase windings and a moving platform. The DLSRM is a second-order control object and the model without load can be represented as follows [22]:

$$\begin{bmatrix} \dot{x}_p \\ \ddot{x}_p \end{bmatrix} = \begin{bmatrix} 0 & 1 \\ 0 & -\frac{b_p}{m_p} \end{bmatrix} \begin{bmatrix} x_p \\ \dot{x}_p \end{bmatrix} + \begin{bmatrix} 0 \\ \frac{1}{m_p} \end{bmatrix} u_p,$$

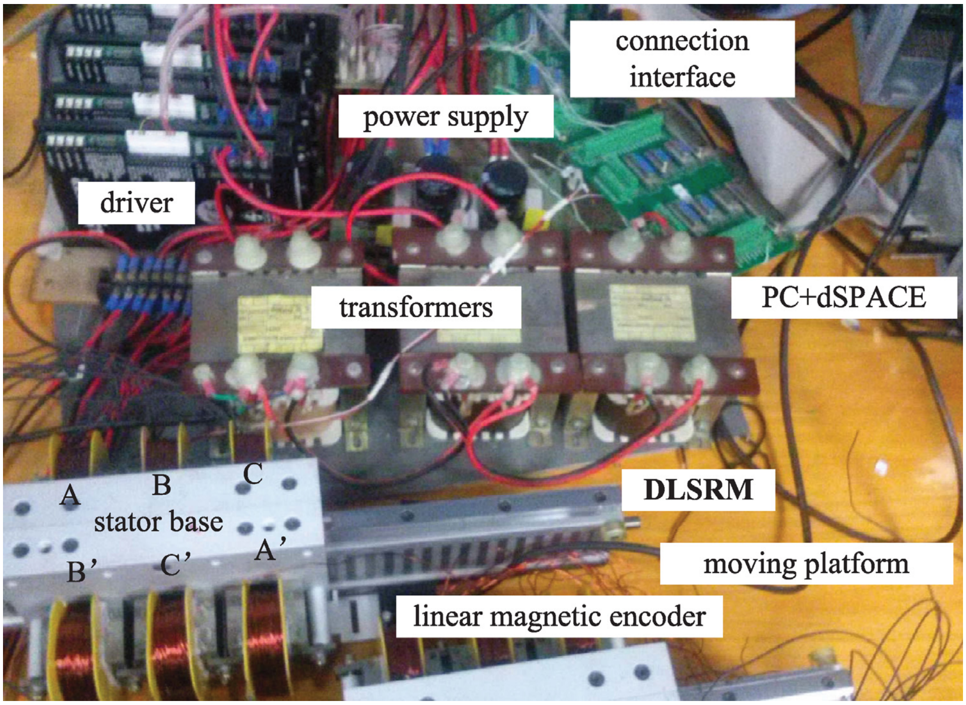

Fig. 9. The experimental platform.

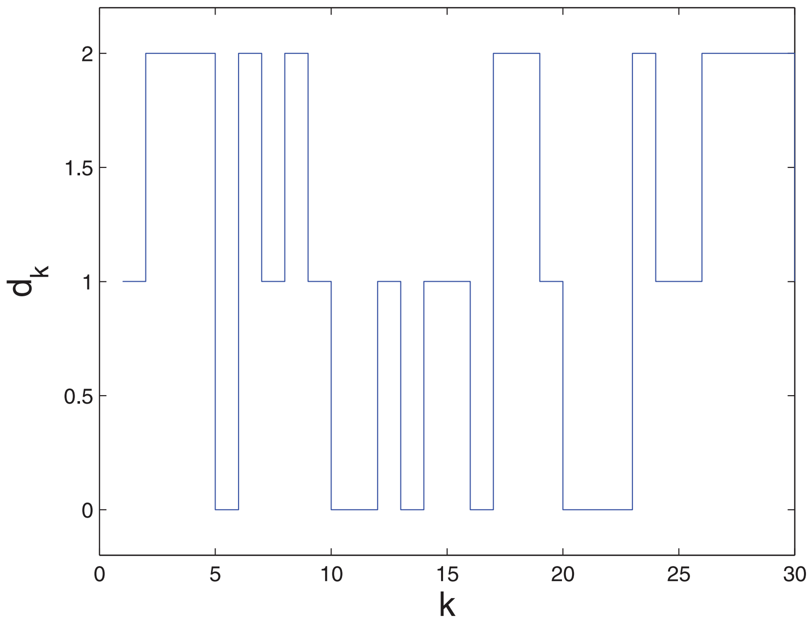

Fig. 10. Time delays d_k.

where x_p denotes the position, m_p is the mass of the moving platform, b_p is the friction coefficient, m_p =1.5 kg and $b_p = 0.5$. System parameters of the DLSRM model can be derived by the discretization with a sampling time of 10 ms:

$$A = \begin{bmatrix} 0 & 1 \\ 0 & -0.3333 \end{bmatrix}, B = \begin{bmatrix} 0 \\ 0.6667 \end{bmatrix}.$$

To apply Theorem 3 in this example, the aforementioned DLSRM system parameters are obtained by online system identification method. Provided the fact that constructing the exact mathematical model of a real time DLSRM system is difficult,

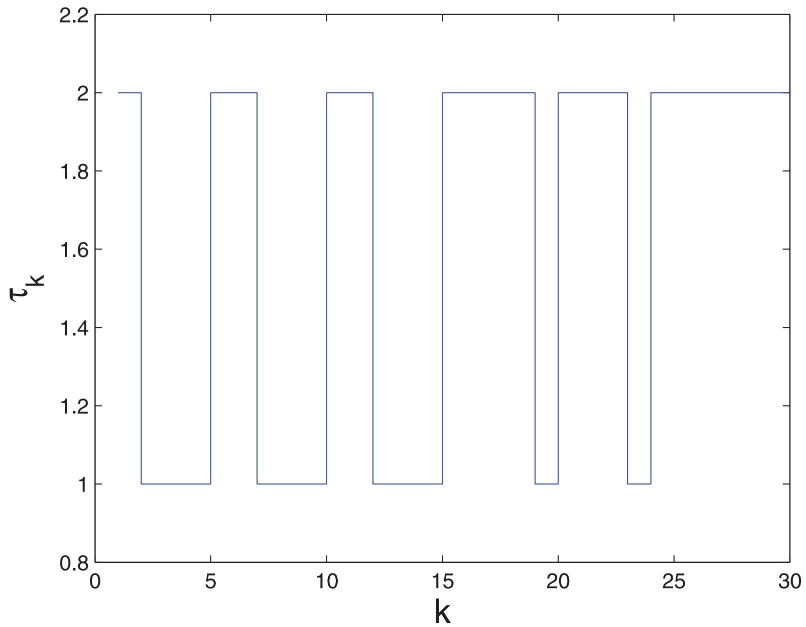

Fig. 11. Time delays τ_k.

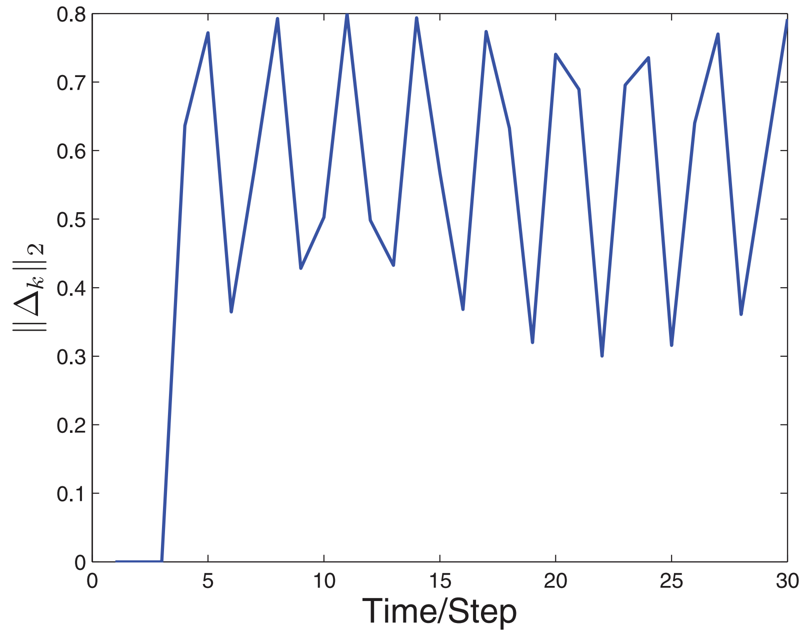

Fig. 12. Values of $\|\Delta_k\|_2$.

parameter uncertainties ΔA and ΔB are introduced. Matrixes D, E_1, and E_2 are given as follows:

$$D = \begin{bmatrix} 0 & 0.3 \\ 0.02 & -0.05 \end{bmatrix}, \quad E_1 = \begin{bmatrix} 0.01 & 0.02 \end{bmatrix}, \quad E_2 = 0.03.$$

The random networked time delays $d_k \in \{0, 1, 2\}$ and $\tau_k \in \{1, 2\}$ and the transition matrices are given by the following:

$$\pi = \begin{bmatrix} 0.1 & 0.5 & 0.4 \\ 0.2 & 0.3 & 0.5 \\ 0.3 & 0.5 & 0.2 \end{bmatrix}, \quad \lambda = \begin{bmatrix} 0.7 & 0.3 \\ 0.4 & 0.6 \end{bmatrix}.$$

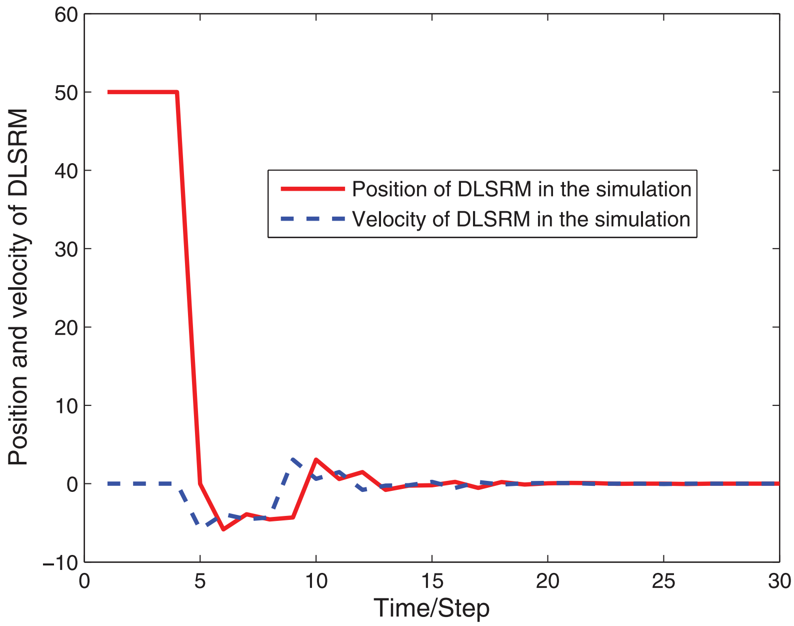

Fig. 13. Simulation Results.

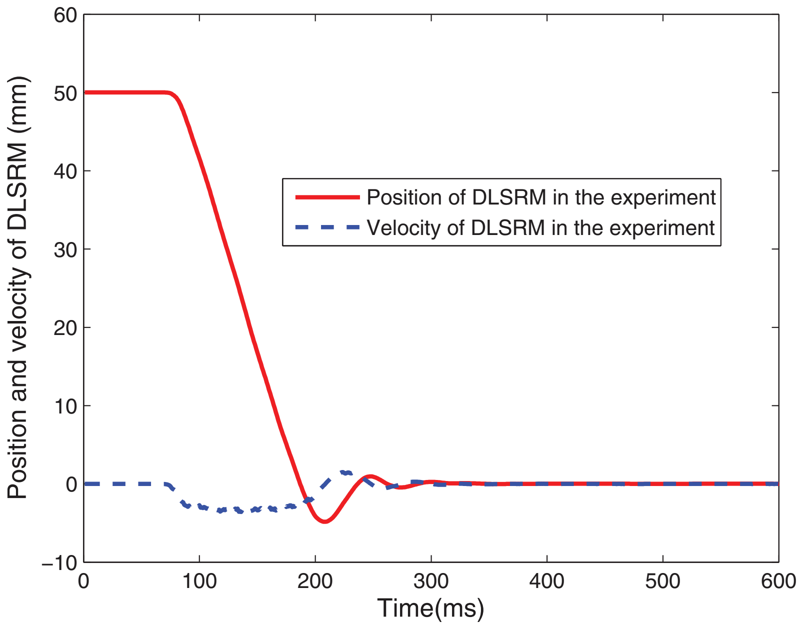

Fig. 14. Experiment Results.

We set the initial values as $x_0 = \begin{bmatrix} 50 & 0 \end{bmatrix}^T$, which denotes the DLSRM location at the position of 50 mm with zero velocity. We set the tuning parameters as $\vartheta_1 = 0.8$ and $\vartheta_2 = 1.1$, respectively. The time-varying norm-bound uncertain parameters Δ_k is assumed as follows:

$$\Delta_k = \begin{cases} \begin{bmatrix} 0.8\sin(k) \\ 0.3\cos(k) \end{bmatrix}, & 4 \le k \le 30 \\ 0, & \text{otherwise.} \end{cases}$$

By applying Theorem 3, we can obtain a scalar $\varepsilon = 0.5224$ and the gain matrix K of the controller (5):

$$K = \begin{bmatrix} -0.1748 & -0.3897 \end{bmatrix}.$$

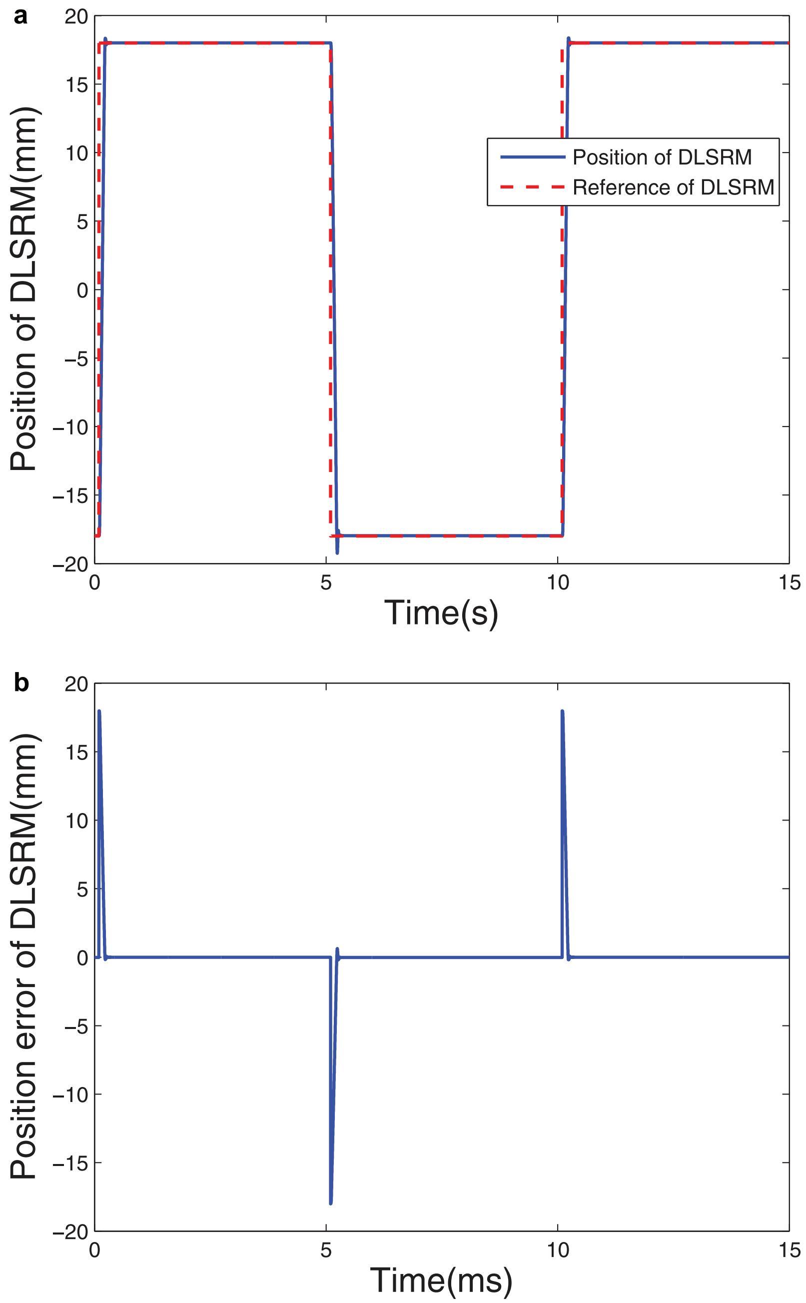

Fig. 15. Response profiles at 18 mm and 0.1 Hz under square reference. (a) Trajectory. (b) The enlarged view of error.

Figs. 10 and 11 illustrate that part of the simulation with random time delays d_k and τ_k are dominated by their corresponding transition probability matrices. Fig. 12 demonstrates the $\|\Delta_k\|_2$ of the time-varying norm-bound uncertain parameter Δ_k and it indicates that $\|\Delta_k\|_2 < 1$. Figs. 13 and 14 demonstrate the simulation and experimental results of the DLSRM system. Figs. 13 and 14 prove that the networked DLSRM system exhibits robust stochastic stability under the robust controller $\bar{u}_k = \begin{bmatrix} -0.1748 & -0.3897 \end{bmatrix} \bar{x}_k$. Figs. 13 and 14 show that the simulation results correspond to the experimental results and both results verify the effectiveness of the proposed control method.

Remark 6. For convenience, the unit for the horizontal axis is step and it represents 10 ms (Fig. 13). Considering the mechanical inertia and initial position of the DLSRM, a time delay exists from the response profiles in the experiment. Figs. 13 and 14 indicate a good agreement between the simulation and experiment.

In order to further validate the proposed method, the position response profiles for the DLSRM system under the square reference signal are provided experimentally as follows.

Due to the mechanical inertia, there is a considerable transient process under the square position reference signal with the amplitude of 18 mm and frequency of 0.1 Hz, as shown in Fig. 15. Although there exhibits sharp overshoots at variable amplitude and frequency values, the position response waveforms quickly converge to the steady states under the square position reference. Due to machine imperfections such as the non-uniform friction or manufacture defects, the response waveforms from the positive and negative transitions are not identical and the maximum absolute steady-state error values from the positive and negative transitions are 2.5 μm and 3 μm, respectively.

Remark 7. Parameters ϑ_1 and ϑ_2 are introduced in Theorem 3. To guarantee the negativeness of block (3,3) in Eq. (10), it is recommended to choose $0 < \vartheta_1 < 1$ and $\vartheta_2 > 1$. When the values of the tuning parameters $\vartheta_1 > 0$ and $\vartheta_2 > 0$ differ, we can obtain K by applying Theorem 3. The values are listed in Table 1. The state response under the different ϑ_1 and ϑ_2 values is

Table 1
Relationship among ϑ_1, ϑ_2, ε, and K.

ϑ_1	ϑ_2	ε	K
0.1	1.1	1.6146	$\begin{bmatrix} -0.0048 & -0.0075 \end{bmatrix}$
0.4	1.4	0.4905	$\begin{bmatrix} -0.0443 & -0.0959 \end{bmatrix}$
0.6	1.6	0.7083	$\begin{bmatrix} -0.0655 & -0.1605 \end{bmatrix}$
0.7	1.7	0.5257	$\begin{bmatrix} -0.0923 & -0.1858 \end{bmatrix}$
0.8	1.2	0.4990	$\begin{bmatrix} -0.1648 & -0.3562 \end{bmatrix}$
0.9	1.3	2.2953	$\begin{bmatrix} -0.1076 & -0.3533 \end{bmatrix}$

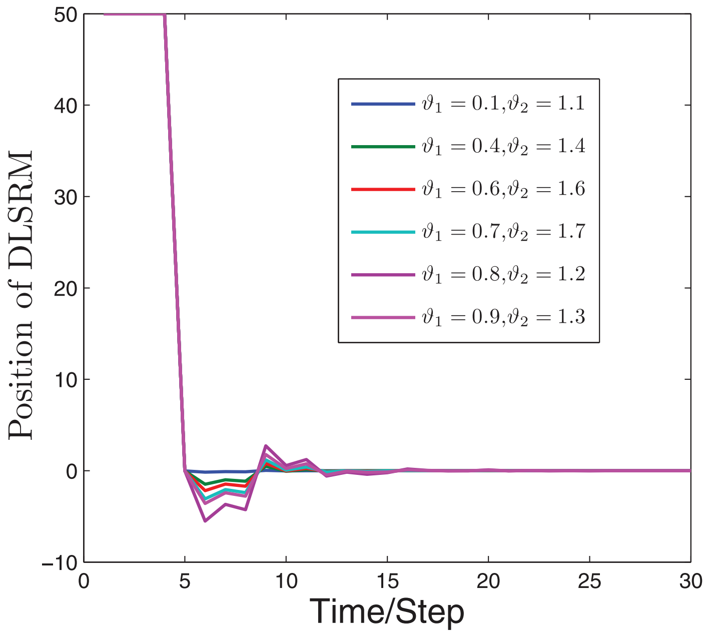

Fig. 16. Response of position.

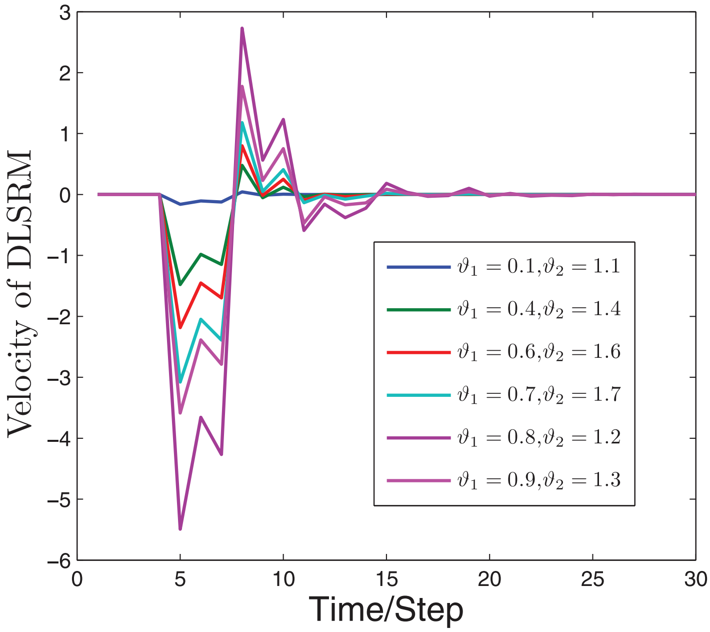

Fig. 17. Response of velocity.

illustrated in Figs. 16 and 17, respectively. These response results do not vary significantly with the variation from ϑ_1 and ϑ_2 values. The simulation results also demonstrate that the proposed method is conservative.

5. Conclusions

In this paper, we have investigated the robust stability problem for the NCS with uncertain parameters and random time delays in both forward and feedback communication links modeled by two Markov chains. The focus of this study is the design of a robust controller to stabilize uncertain NCSs and the application to the DLSRM system over a communication network. By constructing a new Lyapunov functional and using a free-weighting matrix technique, several novel robust stability criteria are derived in terms of LMIs. Simulation and experimental results are provided to demonstrate the effectiveness of the proposed approach on the networked DLSRM based motion control system.

Appendix A. Proof of Theorem 1

Consider a new Lyapunov functional candidate with the following form:

$$V(x_k, d_k, \tau_k) = V_1(x_k, d_k, \tau_k) + V_2(x_k, d_k, \tau_k) + V_3(x_k, d_k, \tau_k), \tag{A.1}$$

where $\forall d_k = i \in \mathbb{M}$ and $\forall \tau_k = m \in \mathbb{N}$,

$$\begin{aligned} V_1(x_k, d_k, \tau_k) &= x_k^T P_{i,m} x_k, \\ V_2(x_k, d_k, \tau_k) &= \sum_{l=k-\eta_k}^{k-1} x_l^T Q x_l + \sum_{\theta=-\bar{\eta}+1}^{-\underline{\eta}+1} \sum_{l=k+\theta-1}^{k-1} x_l^T Q x_l, \\ V_3(x_k, d_k, \tau_k) &= \sum_{\theta=-\bar{\eta}+1}^{0} \sum_{l=k+\theta-1}^{k-1} (\bar{\eta}) \delta_l^T R \delta_l, \end{aligned}$$

with $\eta_k = \tau_k - d_{k-\tau_k}$, $\delta_l = x_{l+1} - x_l$, $\bar{\eta}$, $\underline{\eta}$, $P_{i,\,m}$ Q, and R are defined in Theorem 1. For $d_k = i$, $d_{k+1} = j$, $\tau_k = m$, and $\tau_{k+1} = n$, we denote $\Delta V(x_k, d_k, \tau_k) = \sum_{s=1}^{3} \Delta V_s$.

Let $\xi_k = \begin{bmatrix} x_k^T & \delta_k^T & x_{k-\eta_k}^T & x_{k-\bar{\eta}}^T \end{bmatrix}^T$. For any weighting matrix $\bar{\mathbb{U}}$ with compatible dimensions (and let $\bar{\mathbb{U}} = \begin{bmatrix} \mathcal{U}_1 & \mathcal{U}_2 & \mathcal{U}_3 & 0 \end{bmatrix}$), we have $2\xi_k^T \bar{\mathbb{U}}^T \left((\hat{A} - I) x_k - \delta_k + \hat{B} K x_{k-\eta_k} \right) = 0$ along the trajectory of the solution of the closed-loop system (6) and we obtain

$$\begin{aligned}\Delta V_1 &= \mathbb{E}[V_1(x_{k+1}, d_{k+1}, \tau_{k+1}|x_k, d_k, \tau_k) - V_1(x_k, d_k, \tau_k)]\\ &= \mathbb{E}\Big\{[x_k+\delta_k]^T\bar{P}_{i,m}[x_k+\delta_k]\Big\} - x_k^T P_{i,m}x_k + 2\xi_k^T\bar{\mathbb{U}}^T\Big((\hat{A}-I)x_k - \delta_k + \hat{B}Kx_{k-\eta_k}\Big).\end{aligned} \tag{A.2}$$

$$\begin{aligned}\Delta V_2 &= \mathbb{E}[V_2(x_{k+1}, d_{k+1}, \tau_{k+1}|x_k, d_k, \tau_k) - V_2(x_k, d_k, \tau_k)]\\ &= \Big(\sum_{l=k-\eta_{k+1}+1}^{k} - \sum_{l=k-\eta_k}^{k-1}\Big)x_l^TQx_l + \sum_{\theta=-\bar{\eta}+1}^{-\underline{\eta}+1}\Big(\sum_{l=k+\theta}^{k} - \sum_{l=k+\theta-1}^{k-1}\Big)x_l^TQx_l\\ &= \Big(\sum_{l=k-\underline{\eta}+1}^{k-1} + \sum_{l=k-\eta_{k+1}+1}^{k-\underline{\eta}} - \sum_{l=k-\eta_k+1}^{k-1}\Big)x_l^TQx_l + x_k^TQx_k - x_{k-\eta_k}^TQx_{k-\eta_k} + \sum_{\theta=-\bar{\eta}+1}^{-\underline{\eta}+1}(x_k^TQx_k - x_{k+\theta-1}^TQx_{k+\theta-1})\\ &\le \Big(\sum_{l=k-\eta_k+1}^{k-1} + \sum_{l=k-\bar{\eta}+1}^{k-\underline{\eta}} - \sum_{l=k-\eta_k+1}^{k-1}\Big)x_l^TQx_l + x_k^TQx_k - x_{k-\eta_k}^TQx_{k-\eta_k} + (\bar{\eta}-\underline{\eta}+1)x_k^TQx_k - \sum_{l=k-\bar{\eta}}^{k-\underline{\eta}} x_l^TQx_l\\ &= (\bar{\eta}-\underline{\eta}+2)x_k^TQx_k - x_{k-\eta_k}^TQx_{k-\eta_k} - x_{k-\bar{\eta}}^TQx_{k-\bar{\eta}}.\end{aligned} \tag{A.3}$$

By using Jensen's inequality, we can obtain the following:

$$\begin{aligned}\Delta V_3 &= \mathbb{E}[V_3(x_{k+1}, d_{k+1}, \tau_{k+1}|x_k, d_k, \tau_k) - V_3(x_k, d_k, \tau_k)]\\ &= \sum_{\theta=-\bar{\eta}+1}^{0}\Big(\sum_{l=k+\theta}^{k} - \sum_{l=k+\theta-1}^{k-1}\Big)\bar{\eta}\delta_l^TR\delta_l\\ &= \bar{\eta}^2\delta_k^TR\delta_k - \sum_{l=k-\bar{\eta}}^{k-1}\bar{\eta}\delta_l^TR\delta_l\\ &= \bar{\eta}^2\delta_k^TR\delta_k - \Big(\sum_{l=k-\eta_k}^{k-1} + \sum_{l=k-\bar{\eta}}^{k-\eta_k-1}\Big)(\eta_k+\bar{\eta}-\eta_k)\delta_l^TR\delta_l\\ &\le \bar{\eta}^2\delta_k^TR\delta_k - \eta_k\sum_{l=k-\eta_k}^{k-1}\delta_l^TR\delta_l - (\bar{\eta}-\eta_k)\sum_{l=k-\bar{\eta}}^{k-\eta_k-1}\delta_l^TR\delta_l\\ &\le \bar{\eta}^2\delta_k^TR\delta_k - \Big(\sum_{l=k-\eta_k}^{k-1}\delta_l\Big)^TR\Big(\sum_{l=k-\eta_k}^{k-1}\delta_l\Big) - \Big(\sum_{l=k-\bar{\eta}}^{k-\eta_k-1}\delta_l\Big)^TR\Big(\sum_{l=k-\bar{\eta}}^{k-\eta_k-1}\delta_l\Big)\\ &= \bar{\eta}^2\delta_k^TR\delta_k - \big(x_k - x_{k-\eta_k}\big)^TR\big(x_k - x_{k-\eta_k}\big) - \big(x_{k-\eta_k} - x_{k-\bar{\eta}}\big)^TR\big(x_{k-\eta_k} - x_{k-\bar{\eta}}\big).\end{aligned} \tag{A.4}$$

By combining (A.2), (A.3) and (A.4), we have

$$\mathbb{E}[\Delta V] \le \xi_k^T\Theta_{i,m}\xi_k. \tag{A.5}$$

By using the Schur complement, (8) guarantees $\Theta_{i,\,m} < 0$. Thus, we obtain

$$\mathbb{E}[\Delta V] \le -\lambda_{\min}(-\Theta_{i,m})\xi_k^T\xi_k \le -\beta x_k^Tx_k, \tag{A.6}$$

where $\lambda_{\min}(-\Theta_{i,m})$ denotes the minimal eigenvalue of $-\Theta_{i,m}$,
and $\beta = \inf\{\lambda_{\min}(-\Theta_{i,m}, i \in \mathbb{M}, m \in \mathbb{N})\}$. From (A.6), for any $T \ge 1$, we obtain the following equation:

$$\mathbb{E}[V_{k+1}] - \mathbb{E}[V_0] \le -\beta\sum_{k=0}^{T}\mathbb{E}[x_k^Tx_k]. \tag{A.7}$$

Yielding the following holds for any $T > 1$:

$$\sum_{k=0}^{T}\mathbb{E}[x_k^Tx_k] \le \frac{1}{\beta}[\mathbb{E}[V_0] - \mathbb{E}[V_T]] \le \frac{1}{\beta}[\mathbb{E}[V_0], \tag{A.8}$$

thus implying

$$\sum_{k=0}^{\infty}\mathbb{E}[x_k^Tx_k] \le \frac{1}{\beta}\mathbb{E}[V_0] = \frac{1}{\beta}x_0^TP(d_0, \tau_0)x_0 < \infty.$$

According to Definition 1, implies that the closed-loop system (6) shows stochastic stability, thus completing the proof of Theorem 1.

References

[1] B. Chen, W.A. Zhang, L. Yu, Distributed finite-horizon fusion kalman filtering for bandwidth and energy constrained wireless sensor networks, IEEE Trans. Signal Process. 62 (2014) 797–812.
[2] A. Cuenca, U. Ojha, J. Salt, M.Y. Chow, A non-uniform multi-rate control strategy for a markov chain-driven networked control system, Inf. Sci. 321 (2015) 31–47.
[3] D.J. Du, Q. Bo, M.R. Fei, Multiple event-triggered H_2/H_∞ filtering for hybrid wired-wireless networked systems with random network-induced delays, Inf. Sci. 325 (2015) 393–408.
[4] X.H. Ge, F.W. Yang, Q.L. Han, Distributed networked controlsystems: a brief overview, Inf. Sci. (2015) In press, doi:10.1016/j.ins.2015.07.047.
[5] S.L. Hu, D. Yue, X.P. Xie, Z.P. Du, Event-triggered H_∞ stabilization for networked stochastic systems with multiplicative noise and network-induced delays, Inf. Sci. 299 (2015) 178–197.
[6] G.T. Hui, H.G. Zhang, Z.N. Wu, Y.C. Wang, Control synthesis problem for networked linear sampled-data control systems with band-limited channels, Inf. Sci. 275 (2014) 385–399.
[7] X.C. Jia, X.B. Chi, Q.L. Han, N.N. Zheng, Event-triggered fuzzy H_∞ control for a class of nonlinear networked control systems using the deviation bounds of asynchronous normalized membership functions, Inf. Sci. 259 (2014) 100–117.
[8] X.F. Jiang, On sampled-data fuzzy control design approach for t-s model-based fuzzy systems by using discretization approach, Inf. Sci. 296 (2015) 307–314.
[9] X.F. Jiang, Q.L. Han, On designing fuzzy controllers for a class of nonlinear networked systems, IEEE Trans. Fuzzy Syst. 16 (2008) 1050–1060.
[10] X.F. Jiang, Q.L. Han, New stability criteria for linear systems with interval time-varying delay, Automatica 44 (2008) 2680–2685.
[11] X.F. Jiang, Q.L. Han, S.R. Liu, A. Xue, A new H_∞ stabilization criterion for networked control systems, IEEE Trans. Autom. Control 53 (2008) 1025–1032.
[12] C.L. Lai, P.L. Hsu, The butterfly-shaped feedback loop in networked control systems for the unknown delay compensation, IEEE Trans. Ind. Inf. 10 (2014) 1746–1754.
[13] H. Li, M.Y. Chow, Z. Sun, EDA-based speed control of a networked DC motor system with time delays and packet losses, IEEE Trans. Ind. Electron. 56 (2009) 1727–1735.
[14] H.Y. Li, X.J. Jing, H.R. Karimi, Output-feedback-based H_∞ control for vehicle suspension systems with control delay, IEEE Trans. Ind. Electron. 61 (2014) 436–446.
[15] H.P. Li, Y. Shi, Network-based predictive control for constrained nonlinear systems with two-channel packet dropouts, IEEE Trans. Ind. Electron. 61 (2014) 1574–1582.
[16] J. Lin, K.W.E. Cheng, Z. Zhang, N.C. Cheung, X. Xue, T.W. Ng, Active suspension system based on linear switched reluctance actuator and control schemes, IEEE Trans. Veh. Technol. 62 (2013) 562–572.
[17] D.R. Liu, D. Wang, F.Y. Wang, Neural-network-based online HJB solution for optimal robust guaranteed cost control of continuous-time uncertain nonlinear systems, IEEE Trans. Cybern. 44 (2014) 2834–2847.
[18] J.L. Liu, D. Yue, Event-triggering in networked systems with probabilistic sensor and actuator faults, Inf. Sci. 240 (2013) 145–160.
[19] R.Q. Lu, Y. Xu., A.K. Xue, J.C. Zheng, Networked control with state reset and quantized measurements: observer-based case, IEEE Trans. Ind. Electron. 60 (2013) 5206–5213.
[20] X.L. Luan, P. Shi, F. Liu, Stabilization of networked control systems with random delay, IEEE Trans. Ind. Electron. 58 (2011) 4323–4330.
[21] M.S. Mahmoud, A.-M. Memon, Aperiodic triggering mechanisms for networked control systems, Inf. Sci. 296 (2015) 282–306.
[22] J.F. Pan, Y. Zou, G.Z. Cao, Adaptive controller for the double-sided linear switched reluctance motor based on the nonlinear inductance modeling, IET Electric Power Appl. 7 (2013a) 1–15.
[23] J.F. Pan, Y. Zou, G.Z. Cao, An asymmetric linear switched reluctance motor, IEEE Trans. Energy Convers. 28 (2013b) 444–451.
[24] C. Peng, M.R. Fei, E.G. Tian, Y.P. Guan, On hold or drop out-of-order packets in networked control systems, Inf. Sci. 268 (2014) 436–446.
[25] Z.H. Peng, D. Wang, Y. Shi, H. Wang, W. Wang, Containment control of networked autonomous underwater vehicles with model uncertainty and ocean disturbances guided by multiple leaders, Inf. Sci. 316 (2015) 163–179.
[26] I.R. Petersen, A stabilization algorithm for a class of uncertain linear systems, Syst. Control Lett. 8 (1987) 351–357.
[27] L. Qiu, S.B. Li, B.G. XU, G. Xu, H_∞ control of networked control systems based on markov jump unified model, Int. J. Robust Nonlinear Control 25 (2015a) 2770–2786.
[28] L. Qiu, Y. Shi, F.Q. Yao, G. Xu, B.G. Xu, Network-based robust H_2/h_∞ control for linear systems with two-channel random packet dropouts and time delays, IEEE Trans. Cybern. 45 (2015b) 1450–1462.
[29] L. Qiu, F.Q. Yao, S.B. Li, B.G. Xu, Output feedback guaranteed cost control for networked control systems with random packet dropouts and time delays in forward and feedback communication links, IEEETrans. Autom. Sci. Eng. 13 (2016) 284–295.
[30] D. Quevedo, D. Nesic, Input-to-state stability of packetized predictive control over unreliable networks affected by packet-dropouts, IEEE Trans. Autom. Control 56 (2011) 370–375.
[31] H. Rezaei, R.M. Esfanjani, M.H. Sedaaghi, Improved robust finite-horizon kalman filtering for uncertain networked time-varying systems, Inf. Sci. 293 (2015) 263–274.
[32] Y. Shi, J. Huang, B. Yu, Robust tracking control of networked control systems: application to a networked DC motor, IEEE Trans. Ind. Electron. 60 (2013) 5864–5874.
[33] Y. Shi, B. Yu, Output feedback stabilization of networked control systems with random delays modeled by Markov chains, IEEE Trans. Autom. Control 54 (2009) 1668–1674.
[34] Y. Shi, B. Yu, Robust mixed H_2/h_∞ control of networked control systems with random delays in both backward communication links, Automatica 47 (2011) 754–760.
[35] S.L. Sun, J. Ma, Linear estimation for networked control systems with random transmission delays and packet dropouts, Inf. Sci. 269 (2014) 349–365.
[36] X.M. Tang, B.C. Ding, Model predictive control of linear systems over networks with data quantizations and packet losses quantizations and packet losses, Automatica 49 (2013) 1333–1339.
[37] Y. Tang, H.J. Gao, W. Zou, J. Kurths, Distributed synchronization in networks of agent systems with nonlinearities and random switchings, IEEE Trans. Cybern. 43 (2013) 358–370.
[38] A.A. Waleed, A.A. Marwan, Robust stability of solar-power wireless network control system with stochastic time delays based on H-infinity-norm, Int. J. Syst. Sci. 46 (2015) 896–907.
[39] Y.L. Wang, Q.L. Han, Modelling and controller design for discrete-time networked control systems with limited channels and data drift, Inf. Sci. 269 (2014) 332–348.
[40] X.F. Wang, N. Hovakimyan, Distributed control of uncertain networked systems: a decoupled design, IEEE Trans. Autom. Control 58 (2013) 2536–2549.
[41] Y.L. Wang, T.B. Wang, Q.L. Han, Fault detection filter design for data reconstruction-based continuous-time networked control systems, Inf. Sci. 328 (2016) 577–594.
[42] S.X. Wen, G. Guo, W.S. Wong, Hybrid event-time-triggered networked control systems: scheduling-event-control co-design, Inf. Sci. 305 (2015) 269–284.
[43] B. Xu, Z.K. Shi, C.G. Yang, Composite neural dynamic surface control of a class of uncertain nonlinear systems in strict-feedback form, IEEE Trans. Cybern. 44 (2014) 2626–2634.
[44] F.W. Yang, Q.L. Han, H_∞ control for networked systems with multiple packet dropouts, Inf. Sci. 252 (2013) 106–117.
[45] R.N. Yang, G.P. Liu, P. Shi, C. Thomas, M.V. Basin, Predictive output feedback control for networked control systems, IEEE Trans. Ind. Electron. 61 (2014) 512–520.

[46] X.G. Yang, J.X. Xi, Z.Y. Yu, Stable-protocol admissible synchronizability for high-order singular complex networks with switching topologies, Inf. Sci. 307 (2015) 1–17.
[47] Y.Y. Yin, P. Shi, F. Liu, K.L. Teo, A novel approach to fault detection for fuzzy stochastic systems with nonhomogeneous processes, Inf. Sci. 292 (2015) 198–213.
[48] H. Zhang, P. Cheng, L. Shi, J. Chen, Optimal dos attack scheduling in wireless networked control system, IEEETrans. Control Syst. Technol. (2016) In press, doi:10.1109/TCST.2015.2462741.
[49] L.X. Zhang, H.J. Gao, O. Kaynak, Network-induced constraints in networked control systems-a survey, IEEE Trans. Autom. Control 9 (2013) 403–416.
[50] J.H. Zhang, J. Lam, Y.Q. Xi, Output feedback delay compensation control for networked control systems with random delays, Inf. Sci. 265 (2014) 154–166.
[51] Y. Zhang, H. Ma, Analysis of networked control schemes and data-processing method for parallel inverters, IEEE Trans. Ind. Electron. 61 (2014) 1834–1844.
[52] L.W. Zhang, J.C. Wang, Y. Ge, Robust distributed model predictive control for uncertain networked control systems, IET Control Theory Appl. 8 (2014) 1843–1851.